Feature Extraction Method for Land Consolidation from High Resolution Imagery

RUI GUO[1, 2], DAOLIANG LI [1, 2,*]
1. College of Information and Electrical Engineering, China Agricultural University,
17 Tsinghua East Road, Beijing 100083, P.R. CHINA;
2. Key Laboratory of Modern Precision Agriculture System Integration, Ministry of Education, P.O. Box 209, Beijing, 100083, P.R. CHINA
* Corresponding Author: Email Address: li_daoliang@yahoo.com or dliangl@cau.edu.cn,
Tel: 86-10-62736764; Fax: 86-10-62737741.

Abstract: Land consolidation is a tool for increasing the area of the arable land and improving the effectiveness of land cultivation. With the development of high resolution image, the progress of land consolidation project can be monitored by acquiring information from the image objectively. This paper presents a method to extract the wells and roads in land consolidation project from high resolution images. The well extraction method is based on the gray-level template matching algorithm. The road extraction method is based on mathematical morphology, which is a method for detecting image components that are useful for representation and description. The vector planning maps and high resolution images used to monitor the completion of land consolidation project are registered. The candidate areas are created using the functions of buffer and extraction by mask in GIS. The well template is selected manually from the image. The template is used to find the wells which match the template perfectly. In the road extraction section, Top-hat transform and gray dilation are used to filter the noise of the image. In this way the road feature in the image became wider and even more obvious to be recognized. Then image binarization and thinning algorithm are used to extract the one-pixel centerline of the road. At last, the thinning results are converted to the final vector detection results.

Key-Words: Feature extraction, Mathematical morphology, Template matching, Land consolidation, Remote sensing

1 Introduction

Land consolidation is a tool for improving the effectiveness of land cultivation, land productivity and also the total factor productivity if it induces and enhances technical progress and increases scale economies. Consolidation deals with a large number of phenomena, such as fields, roads, and land use, all of which exhibit characteristic forms and patterns which can be analyzed as to their existing spatial organization, or as to their changing spatial organization through time [1]. With the development of high resolution imagery and the improved feature detection method, remote sensing has become an effective means of land use monitoring.

There are two kinds of algorithm of image matching including gray template matching and feature matching. The gray template matching is about 1 dimension or 2 dimension sliding template which is mainly based on space domain. The differences in this algorithm are the selected template and rules. The feature matching is mainly about extracting points, lines and regions as the bases from the image and then matching. Totally, the gray template matching needs more calculation but more accurate [2]. Lotti and Giraudon[3,4] used a correlation based algorithm with an adaptive window-size that is constrained by an edge map extracted from the image. They presented results on real aerial images. Intille and Bobick[5] presented a stereo algorithm that incorporates the detection of the occlusion regions directly into the matching process. They developed a dynamic programming solution that obeys the occlusion and ordering constraints to find a best path through the disparity-space image. They also used ground control points to eliminate sensitivity to occlusion cost. Xiong et al [6] presented a stereo matching approach which integrates area-based and feature-based processes. Fua[7] described a correlation based multi-resolution algorithm which is followed by interpolation. Anandan[8] described a hierarchical computational frame work for the determination of dense motion fields from a pair of images. A number of researchers have used dynamic programming to solve globallv the matching problem [9, 10, 11, 12, and 13].

The existing road detection approaches cover a wide variety of strategies, using different resolution aerial or satellite images. The approaches are generally classified according to the degree of automation: automatic method and semi-automatic method. Semi-automatic systems assisted by an operator seem to be more effective for road detection now. However, the development trend of road detection is automatic detection system in the near future. After detecting the road network, there may be a few wrong results, which can also be corrected by the system operator. Automatic methods usually detect reliable hypotheses for road segments through edge and line detection and then establish connections between road segments to form road network [14]. Hinz et al. [15] integrate detailed knowledge about roads and their context using explicitly formulated scale-dependent models. The knowledge about how and when certain parts of the road and context model are optimally exploited is expressed by an detection strategy. Mokhtarzade et al. [16] treats the possibility of using artificial neural networks for road detection from high-resolution satellite images on a part of RGB IKONOS and Quick-Bird images from Kish Island and Bushehr Harbor, respectively. Attempts are also made to verify the impacts of different input parameters on network's ability to find out optimum input vector for the problem. A variety of network structures with different iteration times are used to determine the best network structure and termination condition in training stage. Laptev et al. [17] proposed a new approach for automatic road detection from aerial imagery with a model and a strategy mainly based on the multi-scale detection of roads in combination with geometry-constrained edge detection using snakes. It allows for the first time a bridging of shadows and partially occluded areas using the heavily disturbed evidence in the image. Semi-automatic methods require operator to provide some information to control the detection interactively. Most semi-automatic approaches search for an optimal path between a few given points. Gruen and Li et al. [18] and Merlet et al. [19] connect points using dynamic programming, model-driven linear feature detection algorithm based on dynamic programming. Gruen et al. [20] developed linear feature detection method using dynamic programming and LSB-Snakes. They combined characteristics of snakes and Adaptive Least Squares Correlation method. This method might need large computation time on high-resolution images because of its linear systems. Park and Kim [21] presented a road detection algorithm using template matching. But the limitation is that it requires initial seed points on the road central lines and each road segment requires separate seed points. Shukla's scheme is based on the cost minimization technique [22]. The cost is estimated by taking various factors into consideration such as variance, direction, length and width of the road. The process starts with the selection of seed points provided by the user. The approach is called as path following as it follows the path having minimum cost repetitively. Thus the path having minimum cost will be considered as a part of the road. Dal Poz et al. [23] presented a dynamic programming approach for semi-automated road detection from medium- and high-resolution images, proposing a modification of merit function of the original dynamic programming approach, which is carried out by a constraint function embedding road edge properties.

The aim of this paper is to develop an integrate scheme to extract the features to be monitored in land consolidation project which includes a method of well extraction based on template matching and a method of road detection method based on mathematical morphology in land consolidation area. The paper begins with a brief overview of characteristics of the study area. After that the well extraction method is illustrated in detail. This is followed by the road detection flow and the detail algorithm. The algorithm is implemented in the Matlab tools. Results achieved with high resolution satellite image are depicted. Finally, conclusions are drawn.

2 Study Area

The study area is located at 116° 39′ N longitude and 40° 08′ E latitude in the northeast of Beijing (Fig. 1) and is influenced in some parts by different types of land improvement works, such as reclamation, watercourse rectification and land consolidation works, which have a large impact on the rural landscape. This area is characterized by rolling topography and flourishing vegetation. One Quick Bird image, acquired on June 2006, without any clouds/hazes, is used in this study. A Quick Bird image has four multi-spectral bands (i.e. near-infrared (NIR), red, green, and blue) with 2.44-metre spatial resolution and one panchromatic band with 0.61-metre spatial resolution. Both dates of imagery were geo-referenced to a Transverse Mercator projection and Krasovsky spheroid with an RMSE of 1 pixel. It was necessary to radiometrically normalize the multiple dates of remote sensor data even though they were obtained on near anniversary dates.

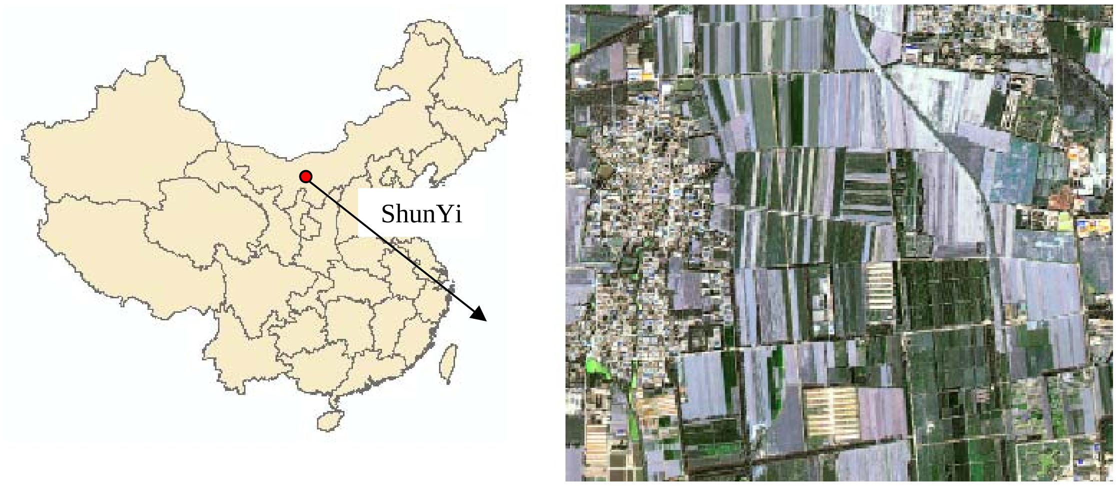

Fig.1. Location of Study Area

3 Well Extraction Scheme

3.1 Gray-level template matching

There are a few kinds of method to describe the gray-level template matching including *Squared difference, Normalized squared difference, Cross correlation, Normalized Cross correlation, Correlation coefficient, Normalized Correlation coefficient*.

If $f(x,y)$ represents $M \times N$ as the original image, then $t(j,k)$ represents $J \times K$ ($J \le M, K \le N$) as the template. While the template $t(j,k)$ moves over the original $f(x,y)$, the region below the template is called sub-image $f^t(x,y)$. When the gray value of template $t(j,k)$ equals the gray value of the sub-image $f^t(x,y)$, the sub-image is the object which we are looking for. In practice when the difference between the two images comes to a threshold value, the sub-image is also the image. The similarity degree between images could be described as *squared difference* as following:

$$SD(x,y)=\sum_{j=0}^{J-1}\sum_{k=0}^{K-1}\left[f^t(x,y)-t(j,k)\right]^2=\sum_{j=0}^{J-1}\sum_{k=0}^{K-1}\left[f(x+j,y+k)-t(j,k)\right]^2 \quad (1)$$

When the $SD(x,y)$ is less, which means the searching image more like the template. The formula (1) can be normalized as *Normalized squared difference*:

$$SDN(x,y)=\frac{\sum_{j=0}^{J-1}\sum_{k=0}^{K-1}\left[t(j,k)-f(x+j,y+k)\right]^2}{\sqrt{\sum_{j=0}^{J-1}\sum_{k=0}^{K-1}\left[f(x+j,y+k)\right]^2}\sqrt{\sum_{j=0}^{J-1}\sum_{k=0}^{K-1}\left[t(j,k)\right]^2}} \quad (2)$$

$SDN(x,y)$ and $SD(x,y)$ can both be used to search the object.

The formula (1) can also be deployed as

$$SD(x,y)=\sum_{j=0}^{J-1}\sum_{k=0}^{K-1}\left[f(x+j,y+k)\right]^2-2\sum_{j=0}^{J-1}\sum_{i=0}^{K-1}t(j,k)f(x+j,y+k)+\sum_{j=0}^{J-1}\sum_{k=0}^{K-1}\left[t(j,k)\right]^2 \quad (3)$$

The third part of formula (3) means the total energy of the template, which is a constant when the template is ensured and is not relative with the (x,y). The first part represents the energy of sub-image, which is changed by (x,y). The second part reflects the relativity between the template and the sub-image, which is also changed by (x,y). When the template and the sub-image are matching, the value comes to the maximum. So *cross correlation* can be used to measure the relativity:

$$C(x,y)=\sum_{j=0}^{J-1}\sum_{k=0}^{K-1}t(j,k)f(x+j,y+k) \quad (4)$$

This can also be normalized as:

$$CN(x,y)=\frac{\sum_{j=0}^{J-1}\sum_{k=0}^{K-1}t(j,k)f(x+j,y+k)}{\sqrt{\sum_{j=0}^{J-1}\sum_{k=0}^{K-1}\left[f(x+j,y+k)\right]^2}\sqrt{\sum_{j=0}^{J-1}\sum_{k=0}^{K-1}\left[t(j,k)\right]^2}} \quad (5)$$

The template described above only use the pixel information which impacts the accuracy. To be more accurate, formula (3) can be modified as

$$R(x,y)=\sum_{j=0}^{J-1}\sum_{k=0}^{K-1}\left(t(j,k)-\overline{t}\right)\left(f(x+j,y+k)-\overline{f}\right) \quad (6)$$

Where

$$\overline{t}=\sum_{j=0}^{J-1}\sum_{k=0}^{K-1}t(j,k)$$

$$\overline{f}=\sum_{j=0}^{J-1}\sum_{k=0}^{K-1}f(x+j,y+k)$$

$R(x,y)$ is called *Correlation coefficient*

$$N(x,y)=\frac{\sum_{j=0}^{J-1}\sum_{k=0}^{K-1}(t(j,k)-\bar{t})\left(f(x+j,y+k)-\bar{f}\right)}{\sqrt{\sum_{j=0}^{J-1}\sum_{k=0}^{K-1}\left[\left(f(x+j,y+k)-\bar{f}\right)\right]^2}\sqrt{\sum_{j=0}^{J-1}\sum_{k=0}^{K-1}\left[(t(j,k)-\bar{t})\right]^2}} \quad (7)$$

But the calculation is huge and is not calculated easily. The total calculation is the following:

$Calculation = RN(x,y) * SearchCount$

So formula (7) could be changed to

$$RN(x,y)=\frac{\sum_{j=0}^{J-1}\sum_{k=0}^{K-1}t(j,k)f(x+j,y+k)-J*K*\bar{t}*\bar{f}}{\sqrt{\sum_{j=0}^{J-1}\sum_{k=0}^{K-1}f^2(x+j,y+k)-J*K*\bar{f}^2}\sqrt{\sum_{j=0}^{J-1}\sum_{k=0}^{K-1}t^2(j,k)-J*K*\bar{t}^2}} \quad (8)$$

$\bar{t}$ and $\sqrt{\sum_{j=0}^{J-1}\sum_{k=0}^{K-1}t^2(j,k)-J*K*\bar{t}^2}$ are const.

3.2 Well extraction algorithm

On the basis of the demand of land consolidation project, the algorithm presents a solution that imports the vector map of the project and registered to the Quick Bird image, which means coarse matching in a traditional way. According to the vector map, the positions of wells to be extracted in the image would be probably estimated. Then template is used to match the wells and correlation coefficient is calculated to search in the buffer distance. This method not only combine the vector map with the project, but has been greatly reduced the calculation of the matching operation. The improving algorithm is as following (Fig.2.):

1. Load the vector map and image of the land consolidation project.
2. Register the vector map and the image to be a coarse matching. After the registration both layers are in the same coordinate system. According to the coarse matching, the vector layer of wells is created. At the same time, attributes of well layer also has been created.
3. Select a well as the matching template image in the image using the AOI tool. Then record the length and width of the template with all bands. If the image has only one band, then calculate the only band in the operation. When the template has more than one band then changes the template image and the sub-image to gray images. Both formulas described are perfect:

$\left(R+G+B\right)/3$ or $0.299*R+0.587*G+0.114*B$

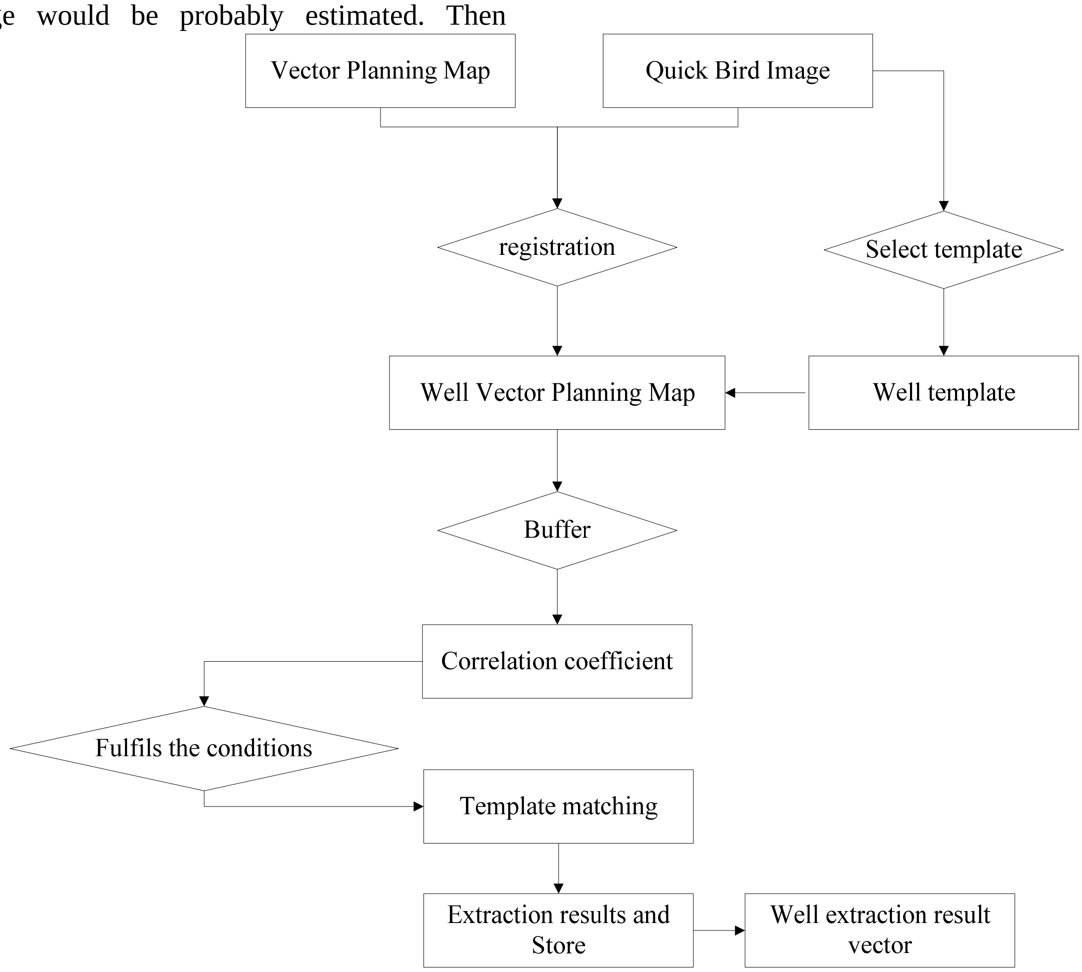

Fig.2. Well Extraction Scheme

4. Get the positions of the wells of vector map and store them in a file. For each position get a rectangle buffer such as 200m. Then glide the template over the buffer region and calculate the correlation coefficient.
5. Set a threshold value of correlation coefficient for each search region. If the calculate value is greater than the threshold then the position is the well to be extracted. The threshold value can be estimated by two knowable templates.
6. For each well that has been matched, create a point layer and check the amount and the positions.

3.3 Results

The reorganization accuracy of the algorithm is limited by the noise of the image, the registration accuracy of maps, the size of template and the correlation coefficient. The buffer distance is 200*200m. The resolution of QuickBird image is 0.61m after image fusion. So the real searching area is 122 * 122 m^2.

We choose two templates and two threshold value to make an experiment as the above algorithm. The two templates are 15 * 16 pixels (template 1)， 10 * 11 pixels (template 2) (See in Fig.3.) There are nine positions of wells that could exist. We use the nine positions to match the wells. The results are described as following table:

Fig.3. Two Kinds of Templates

Table 1: Well Extraction Results

Template / Threshold		Template 1	Template 2
Value 1 (0.70)	Right	1	6
	Wrong	8	3
	Omission	0	0
	Accuracy Rate	11.1%	66.7%
Value 2 (0.80)	Right	3	7
	Wrong	0	1
	Omission	6	1
	Accuracy Rate	33.3%	77.7%

The results listed in the table explain that the extraction accuracy is relative to the size of template and the threshold value. When the value is lower (0.70), there are no omitted wells. But the wrong wells are found. On the contrary, when the value is higher (0.80), there may be some omitted wells. But the right wells are more.

Another factor is the size of the template. When the template is the same size of actual well such as10 * 11 pixels (template 2), the accuracy is higher. When the template is large than the real well, the accuracy is lower. So all illustrations above are the algorithm and flow of well extraction.(See in Fig.4.)

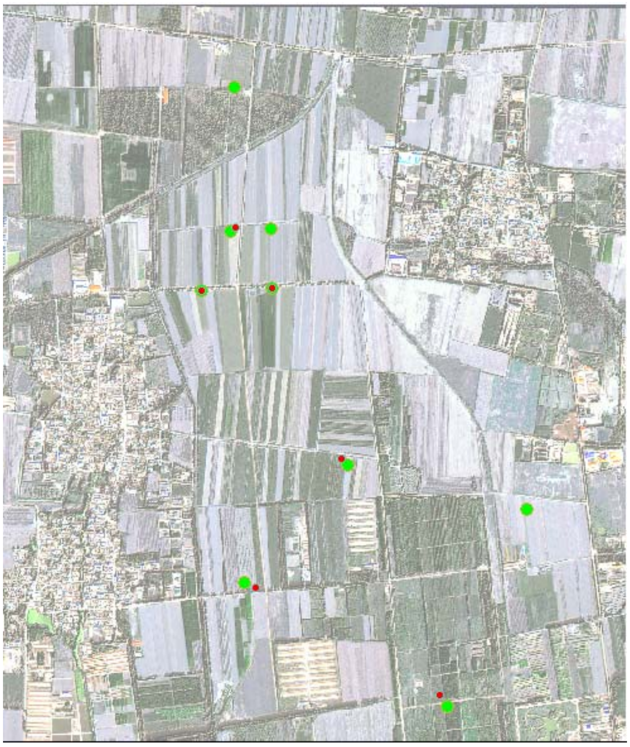

Fig.4. Well Extraction Results

4 Road Detection Scheme

4.1Principle of Mathematical Morphology

Mathematical Morphology is a method for detecting image components that are useful for representation and description. The technique was originally developed by Matheron and Serra [24] at the Ecole des Mines in Paris. It is a set-theoretic method of image analysis providing a quantitative description of geometrical structures. At the Ecole des Mines they were interested in analyzing geological data and the structure of materials. Morphology can provide boundaries of objects, their skeletons, and their convex hulls. It is also useful for many preand post-processing techniques, especially in edge thinning and pruning.

Generally most morphological operations are based on simple expanding and shrinking operations. The primary application of morphology occurs in binary images, though it is also used on grey level images. It can also be useful on range images [25].

4.1.1 Set operations

These transformations involve the interaction between an image A (the object of interest) and a structuring set B, called the structuring element. Typically the structuring element B is a circular disc in the plane, but it can be any shape. The image and structuring element sets need not be restricted to sets in the 2D plane, but could be defined in 1, 2, 3 (or higher) dimensions.

4.1.2 Dilation

Dilation of the object A by the structuring element B is given by

$$A \oplus B = \{x : \hat{B}_x \cap A \neq \varnothing\}$$

The result is a new set made up of all points generated by obtaining the reflection of B about its origin and then shifting this relection by x.

4.1.3 Erosion

Erosion of the object A by a structuring element B is given by

$$A \Theta B = \{x : B_x \subseteq A\}$$

Two very important transformations are opening and closing. Now intuitively, dilation expands an image object and erosion shrinks it. Opening generally smooths a contour in an image, breaking narrow isthmuses and eliminating thin protrusions. Closing tends to narrow smooth sections of contours, fusing narrow breaks and long thin gulfs, eliminating small holes, and filling gaps in contours.

4.1.4 Opening

The opening of A by B, denoted by $A \circ B$, is given by the erosion by B, followed by the dilation by B, that is

$$A \circ B = (A \Theta B) \oplus B$$

4.1.5 Closing

Closing is the dual operation of opening and is denoted by $A \circ B$. It is produced by the dilation of A by B, followed by the erosion by B

$$A \bullet B = (A \oplus B) \Theta B$$

4.2 Road detection algorithm

The flow chart of road detection algorithm is described as the Fig.5. The Quick Bird image and the vector planning map are registered in the same geographic coordinate. The functions of buffer and extraction by mask in GIS are used to obtain the candidate area, which could be used to monitor whether the roads have been built up or the length of the roads. After the candidate area image was created, the filter technique is introduced to emerge the roads. The filter technique contained Top-hat transform and dilation algorithm. Then the histogram of the image was created and threshold could be calculated automatically, which is called binarize image. There might be some parcels of other objects like grass, trees, houses etc. they could be wiped off in terms of shape and area. The thinning algorithm is used and then the roads could be converted to the vector. According to the direction and the length of a road, the tiny lines are also eliminated. After the steps above, the roads are detected.

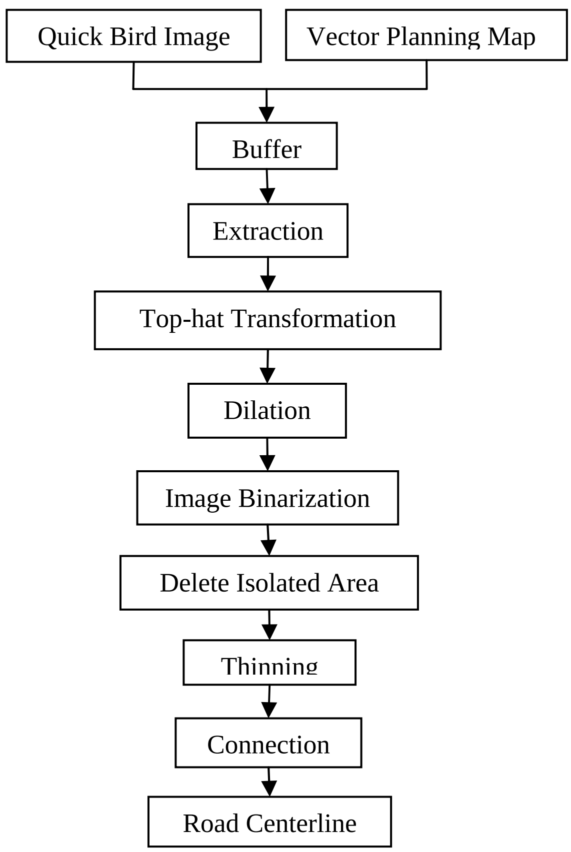

Fig.5. Road detection flow

4.2.1 Generating candidate area

The planning map was edited before the project, according which the roads should be constructed. There may be some roads that were not constructed as plan exactly. The road buffer is created with the width of 30m, in which most roads exist. The buffer then is used as a mask to detect the candidate area. The candidate area is shown in Fig.6.

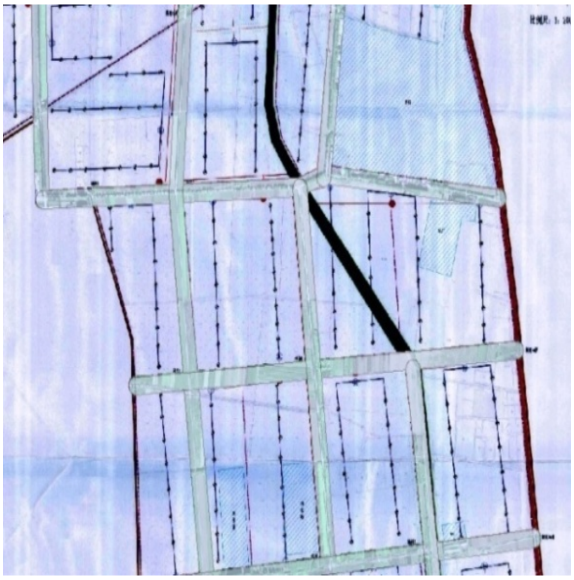

Fig.6. Candidate area

4.2.2 Image filter

In order to smooth the image noise, Top-hat transformation and dilation are used to make the road more recognizable.

The Top-Hat transformation is one of the gray scale morphologic algorithms and is beneficial in finding pixel clusters that are light on a surrounding relatively dark background. It can be used to find neuronal cells in a tissue sample and to detect blood vessels from an image using an X-ray system and fluorescent dyes [26]. This operation is illustrated in Fig.7. The transformation processes original signal f with opening by flat structuring element g. Fig.8 indicates that the peaks are detected as a Top-Hat by subtracting an opened image form the original image.

The opening operation includes two procedures, erosion and dilation. Because the structuring element is flat, the erosion is simplified to find the minimum gray level and the dilation to find the maximum during process. This operation seems to be able to detect the objects above the ground, but unfortunately the detectable size of object depends on the size of the element. Therefore we use this opening operation just to eliminate the peaks, like noise in elevation space [27].

The dilation operation can improve detection quality and accuracy after the Top-hat transformation.

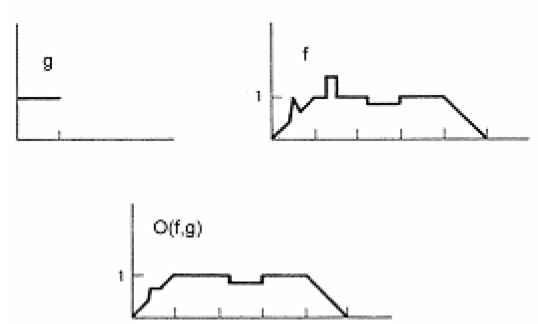

Fig.7. Opening by flat structuring element [Dougherty, 1992]

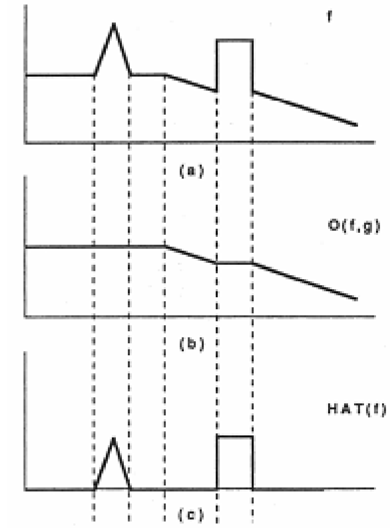

Fig.8. Top-Hat Transformation [Dougherty, 1992]

4.2.3 Image Binarization

Binarization of gray level images after the preprocessing is a special case of segmentation with two labels, which is the most important step of the algorithm. The purpose is simplifying the image to detect the contour. The histogram of this kind of image is described in Fig.9. According to the histogram characteristic, the threshold is calculated exactly as following [28].

From the peak of the image toward the right side:

$$T_1(t) = (p_{t-5} + p_{t-4} + p_{t-3} + p_{t-2} + p_{t-1} + p_t)/6$$

$$T_2(t) = (p_t + p_{t+1} + p_{t+2} + p_{t+3} + p_{t+4} + p_{t+5})/6$$

p_t represents the numbers of point whose gray value is t.

$$\theta(t) = \arctan[(T_1(t) - T_2(t))/6]$$

If $T_1(t) \geq T_2(t)$ *and* $\theta(t) \leq 2 \bullet \frac{\pi}{180}$, t is the threshold. There might be not one t, so the first is just the value.

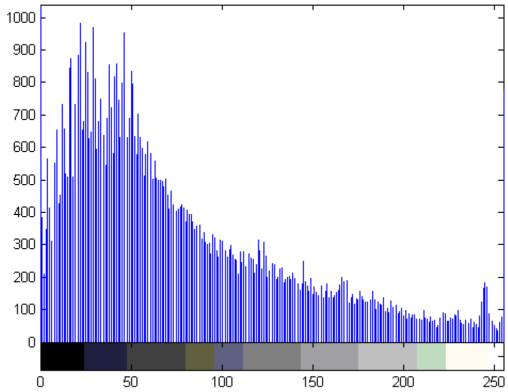

Fig.9. Histogram of image

4.2.4 Delete Isolated Area

There might be a few noise parcels left after the binarization operation, which need to be eliminated. The method is described as following [29]:

(1) Calculate the area a, perimeter p and shape index t of each parcel.

(2) Delete the parcel met the conditions of $a_1 < a < a_2$ and $t > 0.1$, where $r = \sqrt{a/p}$, a means the number of pixel in a parcel and p means the number of pixel in a parcel boundary. a_1 means that the most area of a parcel belong to a road. a_2 means that the most area of isolated parcel.

(3) Direction dilation

After step 2, there are some small parcel left only, but the road is still not connected. So the direction dilation operation is used to connect the discontinuous segment.

(4)Delete the small parcels

4.2.5 Thinning

Thinning is another mathematical morphology operation which can be used to detect the centerline. The general definition of a thinning of a set A by a structuring element S is that we remove from A a part of A specified by the hit-or-miss transform. The thinning is denoted by $A \otimes B$ and may be written in set notation:

$$A \otimes B = A - (A \circledast B)$$
$$= A \cap (A \circledast B)^c$$

The details are described in Fig.10.

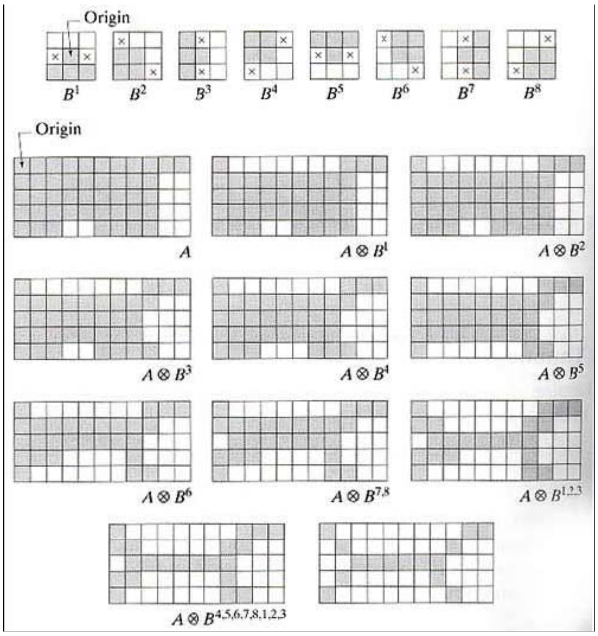

Fig.10.Thinning algorithm

4.3 Results

A piece of candidate area is cut as the test image in Fig.11. The selected candidate area includes typical land consolidation roads. There are also some trees along two sides of the road and the spectrum of some blocks is similar with the road.

Fig.11. A road of study area

Fig.12 shows the original RGB image has been converted to the gray image automatically in Matlab by the function of *rgbtogray*. The roads present white lines, but there still are some trees shade the edges of the roads.

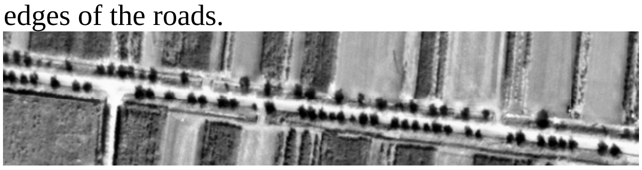

Fig.12. RGB image to gray image

After converting the RGB image to gray image, the roads need to be enhanced and the background needs to be weaken. Fig.13 shows the results after image filter which contain the Top-hat transformation and dilation. The functions in Matlab are *imtophat* and *imdilate*.

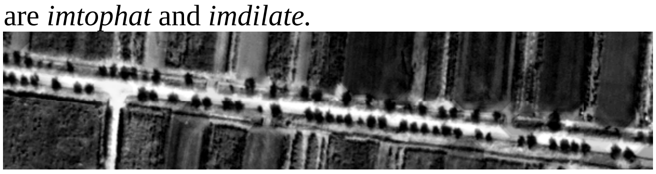

Fig.13. Top-hat transformation

Binarization is the most important step in the whole scheme because it completely differentiates the roads and background. It is a kind of image segmentation, which sets a threshold and divides the image into two parts. The threshold is acquired from the formula described above. Fig.14 and Fig.15 show that the profile of the road to be detected has been come out. The function *im2bw* is used. But there are still some gaps and redundancies.

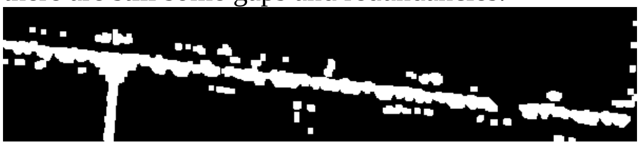

Fig.14. Image Binarization

Fig.15. Deleting Isolated Area

After the connection and thinning operation, the final centreline of road has been detected and is shown in Fig.16

Fig.16. Thinning

Taken together, the final results of road detection scheme have been carried out with a piece of image in ShunYi land consolidation area and the results seem to be good and practical.

6 Conclusion

A method of feature extraction based on gray-level template matching and mathematical morphology for land consolidation has been briefly described. The mathematical morphology is easy to understand and implement. The experiment result on Quick Bird satellite image tells that our method can be one of the solutions for developing fully operational feature extraction system for land consolidation.

The high-resolution images are preferable due to use of width and variance information for road detection. On the other hand, the multispectral information should also be fully used. The concept of semi-automation has shown to be excellent for practical applications, as there is always an editing option when some automation fails due to low image quality, disturbances and other effects, but the automatic method should be the studied in the feature.

Acknowledgement

The research was financially supported by State science and technology support projects (Contract No: 2008BAB38B04).

References:

[1] Wu, Z., Liu, M., Davis, J., Land consolidation and productivity in Chinese household crop production, *China Economic Review*, Vol 16, Issue 1, 2005, pp. 28-49.

[2] Changming. Sun, Multi-Resolution Rectangular Subregioning Stereo Matching Using Fast Correlation and Dynamic Programming Techniques, CMIS Report No. 98/246, CSIRO Mathematical and Information Sciences, Macquarie University Campus, 1998.

[3] J.-L.Lotti, G.Giraudon, Adaptive vvindovv algorithm for aerial image in Proceedings (Jerusalem, Israel)，*International Conference on Pattern Recoanition*, vol. A, pp.701-703, IEEE Computer Society Press, October 9-13 1994.

[4] J.-L. Lotti , G.Giraudon, Correlation algorithm with adaptive window for aerial image in stereo vision, *European Symposium on Satellite Remote Sensing(EUROPTO)*, Rome, Italy, 1994, pp.2315-10.

[5] S.S.Intile, A.F.Bobick, Disparity-space images and large occlusion stereo, *Proceedings of European Conference on Computer Vision*, Stockholm, Sweden, 1994.

[6] Y.Xiong, D.Wang, G.Zhang, Integrated method of stereo matching for computer vision, SPIE Proc, *Application of Digital Image Processing XIX*, Auguest 1996, pp.665-676.

[7] P.Fua, Aparallel stereo algorithm that produce dense depth maps and preserves image features, *Machine Vision Application*, Vol.6, 1993, pp.35-49.

[8] P.Anandan, A computational framework and an algorithm for the measurement of visual motion, *Computer and Information Science*, University of Massachusetts at Amherst, August 1987.

[9] S.A.Lloyd, A dynamic programming algorithm for binocular stereo vision, *GEC Journal of Research*, Vol.3, 1985, pp.18-24.

[10] G.L.Gimel'farb, V.M.Krot, M.V.Grigorenko, Experiments with summarized intensity-based dynamic programming algorithms for reconstructing digital terrain modal, *International Journal of Imaging Systems and Technology*, Vol.4, 1992, pp7-21.

[11] R.Baldwin, H.Yamada, K.Yamamoto, Disparity space and dynamic programming for automatic production of very dense range maps,

Colserange PhoteGrammetry Meets Machine Vision, Vol.1395 September 1990,pp.217-225.
[12] Y.Ohta, T.Kanade, Stereo by intra- and inter-scanline search using dynamic programming, *IEEE Transactions on Pattern Analysis and Machine Intelligence*, Vol PAMI-7, 1985, pp.139-154.]
[13] A.Rojas, A.Calvo, J.Munoz, A dense disparity map of stereo images, *Pattern Recognition Letters*, Vol.18, 1997, pp.385-393.
[14]. Wiedemann, C., Heipke, C., Mayer, H., Hinz, S., Automatic extraction and evaluation of road network from MOMS-2P imagery. *Int. Archiv. Photogrammetry and Remote Sensing*. 32 (Part 3/1), 1998, pp.285–291.
[15]. Hinz, S., Baumgartner, A., Automatic extraction of urban road networks from multi-view aerial imagery. *Journal of Photogrammetry & Remote Sensing*. Vol.58, 2003, pp.83-98.
[16]. Mokhtarzade, M., Valadan Zoej, M.J., Road detection from high-resolution satellite images using artificial neural networks. *International Journal of Applied Earth Observation and Geoinformation*, Vol.9, 2007, pp.32-40.
[17]. Laptev , I., Mayer , H., Lindeberg, T., Eckstein, W., Steger, C., Baumgartner, A., Automatic extraction of roads from aerial images based on scale space and snakes. *Machine Vision and Applications*, Vol.12, 2000, pp.23-31.
[18]. Gruen, A., Li, H., Road extraction from aerial and satellite images by dynamic programming. *Journal of Photogrammetry and Remote Sensing*, Vol.50, No.8, 1995, pp.11-20.
[19]. Merlet, N., Zerubia, J., New Prospects in Line Detection by Dynamic Programming. *IEEE Trans Pattern Anal Mach Intell*, Vol.18, No.4, 1996, pp.426–431.
[20] Gruen, A., Li, H., Semi-Automatic Linear Feature Extraction by Dynamic Programming and LSB-Snakes. *Photogrammetric Engineering & Remote Sensing*, Vol.63, No.8, 1997, pp. 985-995.
[21] Park, S., Kim, T., Semi-Automatic road Extraction algorithm from IKONOS images using template matching . *Proc. 22nd Asian Conference on remote Sensing*, 2001, pp.1209-1213.
[22]. Shukla, V., Chandrakanth, R., Ramachandran, R., Semi-automatic road extraction algorithm for high resolution images using path following approach. In: *Indian Conference on Computer Vision, Graphics and Image Processing*. Ahmadabad, 2002, pp.231-236.
[23] Dal Poz, A. P., do Vale, G. M., Dynamic programming for semi-automated road extraction form medium and high resolution images [J], *International Archives of the Photogrammetry, Remote Sensing and Spatial Information Sciences*, 2003, 34: Part 3 /W8, pp. 87-91.
[24] J. Serra. *Image Analysis and Mathematical Morphology. Academic Press*, 1982.
[25]http://homepages.inf.ed.ac.uk/rbf/CVonline/LOCAL_COPIES/OWENS/LECT3/node3.html
[26] Dougherty, Edward R. 1992. *An Introduction to Morphological Image Processing*, SPIE Optical Engineering Press, Center for Imaging Science Rochester Institute of Technology.
[27] Shao, Y., Chen, L. Object *Segmentation in Elevation Space Using Mathematic Morphology*.
[28] Wang, Yaoge. Road extraction from remote sensing image based on mathematical morphology, *MS Thesis. Dept. of Cartography and Geographic Information Engineering*, Information Engineering University of the People's Liberation Army.
[29] An, R., Feng, X. Road Feature Extract ion form Remote Sensing Classified Imagery Based on Mathematica lM orphology and Analysis of Road Networks. *Journal of Image and Graphics*, Vol.8, 2002, pp.798-804.